IBIMA Publishing
Communications of International Proceedings
https://ibimapublishing.com/p-articles/46AI/2025/4644625/
Vol. 2025 (34), Article ID 4644625

Estimating Measurement Accuracy In Modern Quantum Architectures*

Marek WRÓBLEWSKI and Andrzej OBUCHOWICZ

Institute of Control & Computation Engineering
University of Zielona Góra, Zielona Góra, Poland,

Correspondence should be addressed to: Marek WRÓBLEWSKI, m.wroblewski@issi.uz.zgora.pl

* Presented at the 46th IBIMA International Conference, 26-27 November 2025, Ronda, Spain

Abstract

This article presents the current capabilities for measuring the accuracy of selected IBM Q-class quantum architectures for specific stages and tasks of the recommendation process in hybrid classical-quantum recommendation systems. The main motivations for this research undoubtedly include the increased use of quantum technologies to accelerate the computational process in recommendation systems, as well as the need to assess the utility of available quantum processors for tasks requiring high accuracy. A comparison of the implementation of complex multi-qubit systems in a quantum simulator with that on a real quantum computer is discussed to demonstrate the measurement accuracy of currently available quantum architectures and the error rate compared to simulations of near-ideal systems. The literature lacks consistent comparative analyses that compare real implementations of multi-qubit systems on real quantum computers with their ideal simulations. The existing works mainly focus on model examples or theoretical analyses, which leaves a gap regarding the estimation of the actual error rate and stability of the performed calculations in recommendation applications. This motivated the presentation of important aspects of error generation and the identification of their causes.

Keywords: quantum computer, qubit, quantum circuits, recommendation systems, decoherence

Introduction

One of the most dynamically developing areas of artificial intelligence is quantum computing. The constant development and increase in the number of available qubits means that companies such as IBM, Google, D-Wave, and Rigetti are competitively offering ever-new architectures with increased qubit counts and interconnection methods, significantly improving computational capabilities and the full range of available quantum hardware resources. The continued development of existing algorithms and the implementation of new algorithms, which also optimize resource utilization without the need to adapt each time the circuit is designed, for example, by using the transpiling mechanism in IBM Q systems, delegating the computational component to a quantum coprocessor in hybrid classical-quantum recommendation systems increases the speed of expected predictions [1, 2, 3].

This is because in quantum systems, the basic units of quantum information, called qubits, exist in superposition states, enabling parallel computation. It should be noted that in certain cases, low measurement accuracy may be achieved due to noise, hardware errors, long post-calibration times, or limitations stemming directly from technological constraints related to the way qubits are interconnected and the direct possibility of peer-to-peer communication [4, 5]. Not only in the context of recommendation tasks, final measurement is an essential part of the implementation of the entire hybrid system, as it enables the reading of the final state of the indicated qubits. It should be remembered that this involves irreversible loss of information and the possibility of errors [6,

Cite this Article as: Marek WRÓBLEWSKI and Andrzej OBUCHOWICZ, Vol. 2025 (34) "Estimating Measurement Accuracy in Modern Quantum Architectures " Communications of International Proceedings, Vol. 2025 (34), Article ID 4644625, https://doi.org/10.5171/2025.4644625

7]. This article aims to demonstrate the measurement accuracy for the indicated quantum circuits implemented in real and simulation environments, as well as to identify factors influencing the final quality achieved.

Quantum Preliminaries

The basic unit of quantum information is the qubit. It has basis states

$$|0\rangle = 10, \quad |1\rangle = 01$$

or superpositions of these states: $|\psi\rangle = \alpha|0\rangle + \beta|1\rangle$, where $\alpha, \beta \in C$, $|\alpha|_2 + |\beta|_2 = 1$. Superposition of the indicated quantum states enables parallelization of operations processing the indicated quantum states. Quantum computations are performed using unitary operations represented by quantum gates divided according to the number of qubits they affect. There are single-qubit gates, which include the X, Y, Z, H, S, and T gates, and two-qubit quantum gates such as CNOT and CZ. In the context of the discussed issue, measurement in a standard computational basis for $\{|0\rangle, |1\rangle\}$ causes the collapse of the wave function, where:

$$|\psi\rangle = \alpha|0\rangle + \beta|1\rangle,$$

is the probability of obtaining a result equal to 0 is $|\alpha|_2$, while the result is equal 1 that is $|\beta|^2$. It should be noted that the obtained result is stochastic. This means that to obtain a highly reliable result, the same circuit must be implemented
many times. In IBM Q quantum systems, the number of repetitions is described using the ”shots” parameter [2, 8, 9].

The measurement performed is the effect of the action of the measurement system on the quantum system. The von Neumann measurement operation occurs when the measurement system is macroscopic, i.e., it obeys the superselection rule [10, 11, 12, 13]. The definition of the von Neumann measurement operation is equivalent to the definition of the projective measurement operation, which is described by means of observables that are Hermitian operators acting in the state space of the system being measured [14, 15]. A single observable has a spectral distribution:

$$M = \sum_i \lambda_i P_i, \tag{1}$$

where P_i is the eigenspace projector for the operator M with eigenvalue λ_i. The expression

$$p(\lambda_i) = \langle\psi|P_i|\psi\rangle, \tag{2}$$

represents the probability of obtaining the result λ_i, which causes that after performing a measurement operation on the system, its state is determined as follows:

$$|\Psi_{msrt}\rangle = \frac{P_i|\psi\rangle}{\sqrt{p(\lambda_i)}}. \tag{3}$$

Quantum circuit measurement simulation

As part of the experiment, to assess accuracy and identify differences between simulation and actual circuit implementation, quantum circuits were designed and implemented as part of a complex hybrid classical-quantum recommendation system. For this purpose, two groups of quantum circuits were studied. The first group is responsible for the initialization and encoding of identifiers in the quantum database. Circuits of 20, 25, and 29 qubits were implemented, as this number was dictated by the available RAM allocated to the quantum computation simulator. In the case of the Statevector Simulator, Statevector stores the full state vector of the quantum system, where for n qubits, the state space is represented by a vector of length 2n. Each element of this vector is a complex number (meaning it takes up 16 bytes). Therefore, with 16 GB of RAM, approx-

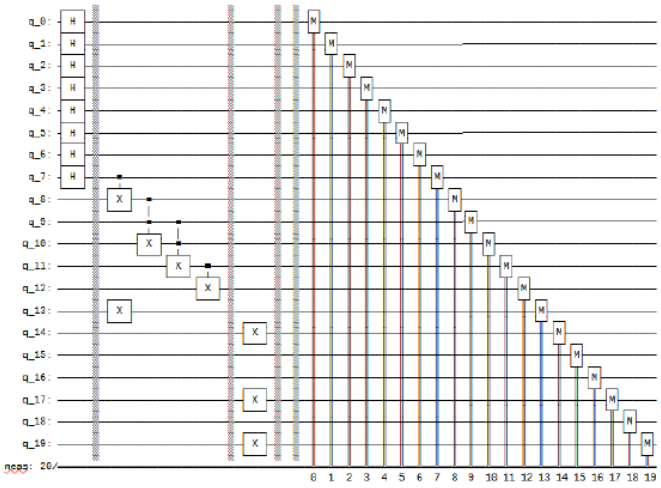

Fig. 1. The circuit is responsible for the initialization process of the quantum database. The first part uses Hadamard gates to allocate identifiers, the second part is responsible for encoding the features of the identifiers stored in the quantum database, and the third part of the circuit contains an encoded leading feature describing, for example, the system user's preference. The whole process culminates in a quantum measurement of all qubits participating in the recommendation process

imately 34–35 qubits can be supported, which in the case of the aforementioned simulator allows for an allocation of 29 qubits. The circuits were initialized using NOT and CNOT gates. The second group is responsible for amplifying the amplitude of the selected feature using Grover's algorithm, where an encoded feature is selected, whose probability amplitude is amplified to the value desired by the recommendation system, as presented in Fig. 2, which shows the circuit and a graph with the amplitude distribution after executing the circuit indicated in Fig. 3.

The Aer Simulator quantum computing simulator was used to perform the simulation calculations. For a 20-qubit circuit, 8 qubits were allocated for database initialization (id), 6 for encoding object features, and 6 for encoding the feature sought by the user, as shown in Fig. 1. The encoded feature specified by the user is 010110. In the 25-qubit circuit, 15 qubits were allocated for initializing the database (id), 5 for encoding the object features, and 5 for encoding the feature specified by the user, where the encoded feature specified by the user is 00110. In the case of the 29-qubit circuit, 19 qubits were allocated for initializing the database (id), 10 for encoding the object features, and 10 for encoding the feature specified by the user, the index of which was described as 0110101110.

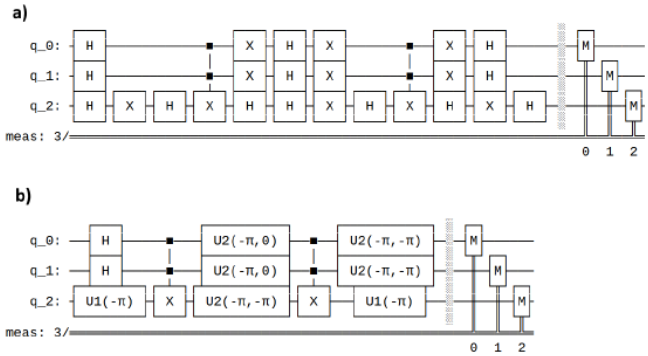

Fig. 2. A graphical implementation of a quantum circuit responsible for implementing the task of amplifying a desired feature with index 100 using Grover's algorithm. Part a) presents the standard circuit form, while part b) presents a circuit form adapted to the indicated real or simulation architecture using a transpiling algorithm, depending on the execution context. The presented case study considers a simulation approach, where the whole process ends with a measurement for each qubit

Measurement accuracy of real quantum computers

To investigate differences in measurements for probability amplitude distributions, a real implementation of the same circuits was performed on the IBM Brisbane quantum architecture. The analysis involved the feature enhancement case using Grover's algorithm with an index of 100. Table Tab. 1 presents selected measures for assessing the performance of the quantum circuit. Data from multiple executions of the same number on a real quantum computer were evaluated. The analysis performed aims to discuss the obtained results using the indicated metrics, referring to the simulation quality and conclusions regarding state distributions and the practical usefulness of quantum computers in recommendation tasks. Interpreting the obtained results, it is noted that the determined

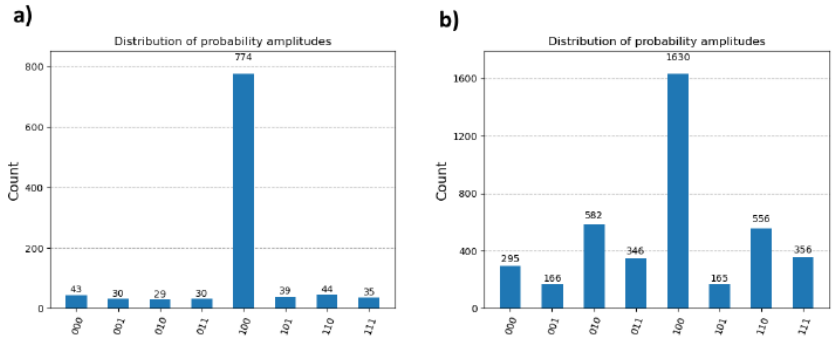

Fig. 3. Comparison of a) simulation and b) actual probability amplitude distribution after the process of amplifying the indicated feature 100 after applying Grover's algorithm

Table 1. Comparison of the values of the measures for the obtained results describing the correspondence of the probability distributions between the Brisbane architecture and the Aer simulator

Type of measure	Value from Brisbane	Value from Aer
MAE	0.164	0.000
MSE	0.042	0.000
Total Variation	0.411	0.000
KL-divergence	1.25	0.000
Hellinger Distance	0.39	0.000
Fidelity	0.53	1.0
Error Rate	0.47	0.0
Entropy	2.35	0.73

Mean Absolute Error (MAE), which measures the average absolute deviation of simulated values from reference values, is 0 for the Aer case, indicating perfect agreement between the simulation and the reference state. In the actual case, the MAE is 0.164, indicating moderate deviation. Interpreting the Mean Squared Error (MSE) for the simulation case reaches 0, indicating the absence of significant squared deviations. In the case of the Brisbane coprocessor implementation, this coefficient is 0.042. This demonstrates the sensitivity of the system to single significantly different values of the probability amplitude for the indicated index. Total Variation measures the maximum difference between the distributions in each category. Aer achieved a value of 0, indicating an ideal distribution, while the actual performance showed a value of 0.411, representing a 41% difference in the probability distribution. This is a significant deviation indicating ambiguity in the representativeness of real data, the indication of which could refer to information derived, for example, from a classical database, which has a significant impact in hybrid classical-quantum recommendation systems. Using KL-divergence, it is possible to measure so-called "lost information" by approximating one distribution to another.

The simulation in Aer achieves a value of 0, which naturally indicates that the distribution resulting from the simulation perfectly matches the reference value. Compared to Brisbane, the KL value is 1.25, suggesting information loss when modeling the actual distribution with simulation. Despite implementing mechanisms

reflecting real factors influencing the environment of the quantum system, the simulator does not capture all the detailed changes currently occurring that affect the amplitude distribution. Hellinger Distance is a measure of the distance between distributions, taking into account the geometric similarity of probability vectors. Aer reaches a value of 0, while Brisbane reaches 0.39, suggesting a slight difference in the distribution of simulated probability amplitudes compared to the actual one. Using the Fidelity measure, it is possible to measure the degree of agreement between distributions on a scale from 0 to 1. A value of 1 indicates complete agreement, while 0 indicates no agreement. The simulator naturally demonstrates complete agreement, obtaining a score of 1, indicating a perfect match, while the actual implementation in Brisbane = 0.53, indicating that the execution process in the actual coprocessor in the indicated architecture reproduces only about half of the features of the actual distribution. The Error Rate indicates the percentage of incorrectly reproduced events. A simulation value of zero again confirms the absence of deviations, while in the case of the actual implementation, the error value of 0.47 clearly indicates that almost half of the events are not identically represented in terms of the assumed accuracy. Using entropy, it is possible to measure the degree of dispersion of the distribution and the amount of uncertainty in the data. The simulation of the distribution achieves a low entropy value compared to the Brisbane simulation, which has a value of 2.35, indicating a higher entropy and thus a more diverse, dispersed distribution of the obtained probability amplitude values.

Summary

The error rates indicate imperfections in the analyzed quantum architecture. However, the obtained results clearly point to a specific index because this amplitude is the largest, confirming the practicality of applying quantum technology to recommendation tasks. It should be noted that the simulator reproduces the results consistently and unambiguously. Using the Brisbane architecture, the execution reflects a portion of the actual distribution of probability amplitude values. In particular, deviations in high-probability states, which are a feature with an index amplified during the execution of Grover's algorithm, lead to a significant difference in the obtained measures. It is worth noting that uncertainty exists in the case of the remaining unamplified probability amplitudes, as from the perspective of recommendation tasks, this distribution is uncertain and highly stable. In this case, it is important to assess the quality of the currently available quantum architecture against data from the Aer simulator. Due to quantum noise and the phenomenon of state decoherence occurring in the physical system, qubits lose their ability to maintain superposition due to interactions with the environment and the preservation of the originally assigned post-calibration values, for example, due to interaction with the electromagnetic field on the chip.

This results in the amplitudes for the measured states ”smearing out.” Furthermore, calibration errors, hardware limitations described in the form of incomplete utilization of interqubit connections, and noise occurring directly on the quantum gates used in the implementation of circuits have a direct impact on the measurement result, thus leading to errors contained directly in the final measurement of the circuit. This is addressed through the continuous development of quantum coprocessor architecture and topology, as well as the development of software and algorithms supporting the circuit implementation process, optimizing its execution within the given quantum architecture [16, 17, 18, 19].

References

- Vasiliu, L., Pop, F., Negru, C., Mocanu, M., Cristea, V., Kolodziej, J., A Hybrid Scheduler for Many Task Computing in Big Data Systems. International Journal of Applied Mathematics and Computer Science, Vol. 27, 2, 385-399 (2017).
- IBM Q platform, https://quantum.ibm.com/, last accessed - september (2024).
- IBM Q Development & Innovation Roadmap, IBM, (2024).
- IBM Q Research, https://research.ibm.com/quantum-computing, last accessed - september (2024).
- Chen, T., Ding, H., et. all., Direct Probe of Topology and Geometry of Quantum States on IBM Q, arXiv preprint arXiv:2403.14249, (2024).
- Cross, A., The IBM Q experience and QISKit open-source quantum computing software, APS March meeting abstracts, vol. 2018, pp. L58–003, (2018).
- Linke, N.M., Maslov, D., Roetteler, M., et. all., Experimental comparison of two quantum computing architectures, National Acad Sciences, vol. 114, 13, pp. 3305–3310, (2017).
- Nielsen, M., Chuang, I., Quantum computation and quantum information, Cambridge University Press, New York (2000).

- Bengtsson, I., Z˙ yczkowski, K., Geometry of Quantum States: An Introduction to Quantum Entanglement, Cambridge University Press, Cambridge (2017).
- Brylinski, K., Chen, G., Mathematics of Quantum Computation, Chapman and Hall/CRC Press, (2002).
- Steeb, W-H., Hardy, Y., Problems and Solutions in Quantum Computing and Quantum Information 4th Edition, World Scientific Publishing Co Pte Ltd,(2018).
- Wightman, A., Superselection rules; old and new, Il Nuovo Cimento B (1971-1996), Vol. 110, No. 5, pp. 751-769, (1995).
- Jacak, L., Quantum computer: a new challenge for nanotechnology, Postepy fizyki, Vol. 53, pp. 72-78, (2002).
- Schutski, R., Lykov, D., Oseledets, I., Adaptive algorithm for quantum circuit simulation, Physical Review A, Vol. 101, 4, pp.042335, APS, (2020).
- Garcia, J., Mandelbaum, R., Davis, R., Janechek, J., Letzter, R., Harishankar, R., Thorpe, L., Murphy, M., Cases Quantum Use., IBM and Daimler use quantum computer to develop next-gen batteries, Quantum, (2023).
- Sanchez-Rivero, J., Talav´an, D., Garcia-Alonso, J., Ruiz-Cort´es, A., Murillo, J.M., Automatic generation of an efficient less-than oracle for quantum amplitude amplification, 2023 IEEE/ACM 4th International Workshop on Quantum Software Engineering (Q-SE), pp. 26–33, IEEE, (2023).
- Bae, J-H., Alsing, P.M., Ahn, D., Miller, W.A., Quantum circuit optimization using quantum Karnaugh map, Scientific reports, Vol. 10, 1, pp.15651, Nature Publishing Group UK London, (2020).
- Venturelli, D., Do, M., Rieffel, E. and Frank, J., Compiling quantum circuits to realistic hardware architectures using temporal planners, Quantum Science and Technology, Vol. 3, No. 2, pp. 025004, (2018).
- Brukner, C., On the quantum measurement problem, Quantum [Un] Speakables II: Half a Century of Bell's Theorem, pp. 95-117, (2017).